# PLASMATRON SIMULATION OF MHD-CHANNEL CONDITIONS*

V. Goldfarb, V. Hruby, and R. Kessler
Avco Everett Research Laboratory, Inc.
2385 Revere Beach Pkwy., Everett, MA, U.S.A.

## ABSTRACT

Laboratory-scale facility with an arc plasma heater and scaled-down version of a slagged wall MHD-channel has been investigated. Thermophysical and optical measurements of temperatures, heat flux, flow velocity and erosion rate show that local conditions in electrode boundary layer of the channel are well simulated.

## 1. INTRODUCTION

A study of plasma flows in slagged wall channels is of interest in relation to coal-fired MHD generators and plasma-metallurgical reactors. An arc heater is a convenient device to generate plasma and particle flows in power-limited experiments where flexibility in gas enthalpy and composition is desirable.

Characteristics of a laboratory-scale facility for investigation of MHD-related problems are presented. Measurements were performed to estimate feasibility of a modeling experiment and of some diagnostic methods.

## 2. EXPERIMENTAL FACILITY

The facility consists of an arc plasma generator, a test section, 100 kW DC power supply, water cooling system (10 atm, 1 ℓ/sec) gas system (liquid nitrogen tank bottled gases), powder supply (Vibrascrew feeder) and diagnostic instrumentation. The plasma generator (Fig. 1) has a 12 mm diameter channel formed by copper rings, with tungsten cathodes and copper-tungsten anodes. Part of the powder introduced in the nozzle forms a liquid slag layer on the surface of a graphite insert. The slag flows into the test section which is a scaled-down version of an actual MHD channel. Two walls of the rectangular channel consist of rows of electrodes separated by insulators. These walls contain replaceable elements so that various metals and ceramics could be tested. Transverse electrical discharge between the walls was produced by a separate rectifier. In experiments described here, one wall was replaced by a copper plate with a gas-protected viewing window. A U-shaped graphite insert was used to restrict the flow cross-section and to increase heat flux to the electrodes. Auxiliary graphite cathode was introduced to provide transverse current to the opposite anodes.

*This work was supported by the United States Department of Energy under Contract DE-AC01-80-ET15614.

## 3. DIAGNOSTIC METHODS AND RESULTS

The range of operating conditions is shown in Table 1, where the data of the last column corresponds to the regime used for thermophysical and optical measurements. These are described later. Data in Table 2 were obtained by standard techniques. Flow velocity was obtained from Pitot tube measurements in the flow core, where the dynamic pressure profile is essentially flat. Heat flux, measured by calorimetry, is substantially reduced by partial or complete coverage of the walls by slag. This is partly due to a decrease of radiative flux from the surrounding graphite walls and partly due to reduced temperature difference between the wall and the gas. A transverse discharge of 1 $A/cm^2$ contributes noticeably to the heat transfer. Heat flux decreases along the channel (from electrode No. 2 to electrode No. 7) by 25%. The precision of electrical conductivity data is low because of the uncertainty in transverse discharge geometry.

Reliability of the data obtained by optical methods (see Tables 3 and 4) depends on fulfillment of the partial LTE assumption. The population density of KI levels does not precisely follow the Boltzmann distribution even for comparatively high quantum numbers (see Fig. 2). The electron density derived by extrapolation of the Boltzmann plot to the ionization limit corresponds to conductivity which is substantially higher than measured. A possible explanation is that optical data characterizes mainly the core flow.

The very high temperature obtained from CuI, TiI and Ca lines may be explained by deviation from equilibrium for levels distanced from ionization limit (by analogy with KI levels). The potassium concentration is deduced from the Saha equation under the hypothesis that its ionization is the only source of free electrons. If ionization of other metals contributes in electron number density, the potassium concentration is overestimated.

Limited information about particulates could be obtained from continuum radiation. Unlikely high particle "colour" temperature could be understood by deviation from black body radiation: emissivity of submicron particles increases with frequency. Concentration of particulate matter in the flow was estimated by measuring absolute continuum intensity and accepting emissivity of 0.5 which is typical for oxides. The result depends on particle size distribution. Large (10μ) particles must be present in a quantity that exceeds mass of the introduced powder even at accepted high temperature (3100K). Evidently, the flow includes sufficient number of smaller particles.

Metal vapors in the flow are produced by evaporation of particulate matter and of the slag layer. The concentration of metals was estimated from relative intensities of KI lines and spectral lines of these metals. The main error in these estimates is due to uncertainty in the excitation temperature. Data in Table 4 is deduced for T = 3200K. There is no correspondence between the metal concentration in vapor phase and metal com-

pounds concentration in a powder. This is not surprising because of large difference in volatility.

Atomic absorption was used to measure the instantaneous rate of anode erosion under the combined influence of heat, slag and electrical current. Usual technique of erosion measurement (by weight) requires disassembling of the channel and only average data with respect to number of coulombs is obtained. Actually erosion increases sharply with current in separate electrode spots, therefore temporal and spacial resolution are of importance. Data of Table 5 shows that anode erosion is detected by measuring atomic absorption at the exit of the test section. Simultaneous recording of absorption in CuI 3274, Pt I 3065 lines and electrical current shows close correlation between current and erosion rate. Emission measurements were also used for erosion monitoring. In this case, radiation from small arcs in the electrode boundary layer was measured to compare copper, gold and silver (last two used as braze material) erosion at various conditions. Radiation originating from these arcs could be distinguished from radiation from the main flow on the basis of high excitation temperature (CuI lines, for instance, are characterized by T = 5200K in case of single 5 ampere electrode arc).

## 4. CONCLUSIONS

The laboratory-scale facility based on the arc heater permits simulation of some features characteristic of the MHD-channel with respect to heat flux, electrode-slag and electrode-current interaction. This simulation could be made closer if a magnetic field were applied and the gas were to include combustion products. Electrical gas heating and the small size of the test section lead to some special electronic properties of the flow, specifically to the deviation from LTE. Emission and absorption optical methods proved to be useful in obtaining flow properties and erosion characteristics. Some of them could be used at real MHD installation for operational control.

TABLE 1

Characteristic Data for Arc Heater Operation

| | Operation Range | Nominal Value |
|---|---|---|
| Mass flow ($gs^{-1}$): Argon | 0.6...1 | 0.8 |
| Nitrogen (main) | 2...4 | 3.2 |
| Nitrogen (transport) | 1...2 | 1.7 |
| Powder ($K_2SO_4$ + Ash) | 0.04...0.2 | 0.15 |
| Arc voltage (V) | 150...260 | 230 |
| current (A) | 170...220 | 200 |
| power (kW) | 25...55 | 46 |
| Plasmation efficiency (%) | 45...52 | 46 |
| Enthalpy ($kJg^{-1}$) | 3.2...4.8 | 3.8 |
| Average Temperature (K) | 2700...3900 | 3100 |

TABLE 2

Characteristic Data for Test Section Flow
(at Electrode No. 3)

| | |
|---|---|
| Flow velocity ($ms^{-1}$) | 280 |
| Heat flux to anode ($Wcm^{-2}$) | |
| without slag and current | 170 |
| with slag | 130 |
| with slag and current | 137 |
| Copper anode temperature (K) | |
| water cooled | 700 |
| nitrogen cooled | 1100 |
| Electrical conductivity W, ($mho \cdot m^{-1}$) | |
| with seed | 10-13 |
| Slag temperature (K) | 1750 |
| Slag flow velocity ($cms^{-1}$) | 2-4 |

TABLE 3

Flow Parameters Measured by Different Optical Methods

| | |
|---|---|
| Electron number density ($cm^{-3}$): | |
| KI (8d, 10s) lines Stark broadening | $<3.10^{-4}$ |
| KI levels population density | $4.10^{14}$ |
| Temperature (K) | |
| Relative intensities of KI lines | 3200 |
| CuI lines | 4200 |
| TiI lines | 4100 |
| Intensity ratio of CaI/CaII lines | 3500 |
| Potassium concentration ($cm^{-3}$) | $1.2 \cdot 10^{15}$ |
| Particles "colour" temperature (K) | 3500 |
| Particles (1-10μ) concentration ($cm^{-3}$) | $10^{5}$-$10^{4}$ |

TABLE 4

Concentration of Metals in Plasma Flow

| Metal | Concentration (% by volume) | Relative Concentration of Metal Compounds in (Seed + Ash) Powder (%) |
|---|---|---|
| Potassium | 0.6 | 70 |
| Aluminum | 0.004 | 7 |
| Iron | 0.07 | 5 |
| Titanium | 0.003 | 0.25 |
| Magnesium | 0.7 | 0.05 |
| Calcium | 0.15 | 1 |
| Copper | 0.25 | * |
| Silicon | * | 12 |

*no data



TABLE 5

Channel Electrode Erosion Measurements

| Type of Electrode | Discharge Current Density ($A/cm^2$) | Average Current per Anode Spot (A) | Light Absorption (%) | Erosion Rate mg/coulomb | Metal Concentration in flow ($cm^{-3}$) |
|---|---|---|---|---|---|
| Copper Anode | 0.5 | 0.07 | 5 | 20 | $\sim 10^{13}$ |
| | 2 | 2 | 60 | 200 | $\sim 10^{14}$ |
| Platinum Anode | 0.5 | 0.07 | 2 | <2 | $< 2.10^{12}$ |
| | 3 | 1.5 | 12 | 10 | $\sim 10^{13}$ |

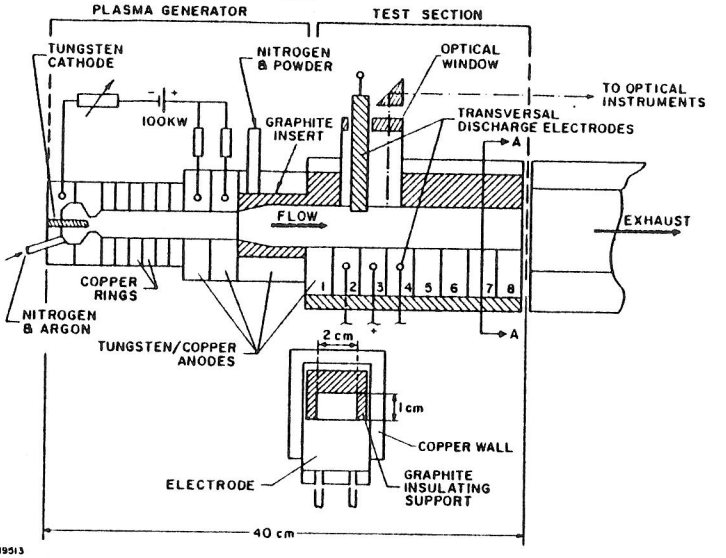


Fig. 1 Schematic of plasma generator and test section

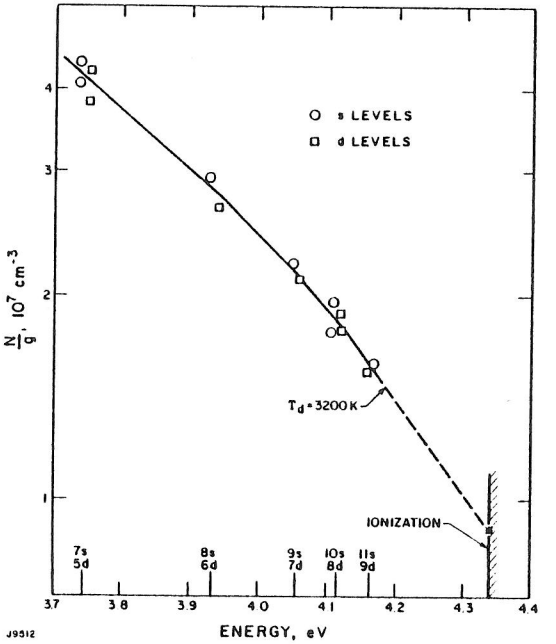


Fig. 2 Population densities of potassium levels